QUANTITATIVE FRACTOGRAPHY MARKERS FOR DETERMINING FATIGUE CRACK GROWTH RATES IN ALUMINIUM AND TITANIUM AIRCRAFT STRUCTURES

M. McDonald *, R. Boykett *, M. Jones *
*Defence Science and Technology Organisation, **QinetiQ Australia
marcus.mcdonald@dsto.defence.gov.au

Keywords: metal fatigue, crack growth, fracture surface markers

Abstract

The determination of fatigue crack growth rates in metallic airframes by quantitative fractography is pertinent for damage tolerance assessments. This has previously been unviable for titanium because of its microstructure, which is relatively difficult to mark distinguishably. Special 'marker' load sequences were developed to create optically reflective imprints on titanium fracture surfaces. The fatigue life effect of the marker loads was minimised while maintaining marker visibility across a broad range of crack sizes. 'Bar-codes' were added to the markers to help positively identify the time progression of the crack growth. The application of a bar-coded marker load sequence technique to element, component and potentially full-scale airframe life substantiation tests would provide additional knowledge about the crack growth conditions at fatigue critical locations in an airframe. This enables a more accurate post-test interpretation (root cause analysis) and improvements to fatigue models; leading to more effective, efficient and timely production changes, retrofits and/or repairs to aircraft structures.

1 Introduction

The determination of crack growth rates in metallic materials is essential for damage tolerance assessments of fatigue cracking in airframe components. Reading the microscopic deformations 'recorded' on the fracture surface of a metal fatigue failure, or Quantitative Fractography (QF), can reveal information about the rate at which the fatigue crack grew under the applied flight loading [1]. This is done by destructively opening up the cracked component and, under the microscope, associating the fracture surface deformations with individual flight manouevre events, thus enabling a plot of the crack size against flight hours to be generated.

QF data is not always easy to obtain since different metals and flight load sequences have different propensities for creating visible fracture surface deformations. The use of special 'marker' load sequences, inserted amongst the usual flight loads, is a relatively common technique for increasing the reliability of QF [2]-[5]. While markers for aluminium have been used occasionally in airframe fatigue tests [6]-[14], markers for titanium are not well developed [10]-[13]. This may be partly due to the microstructure of titanium, for which it can be relatively difficult to produce distinguishable marks [10].

A recent joint study by DSTO[1] & NLR[2] on aluminium [10] showed that the deformations can be made more visible by forcing the crack path to change direction to create a microscopic light reflector on the fracture surface at a particular point in the flight spectrum.

In this work, this concept was developed further to apply to a titanium alloy. Tests were

---

[1] Defence Science & Technology Organisation, Australia
[2] National Aerospace Laboratory of the Netherlands

conducted to assess the visibility and the fatigue life effect of the marker load sequence. Finally, marker 'bar-codes' were developed to help identify the time progression of the crack growth.

2 Experiment Methodology

The marker bands were developed using an iterative methodology based on fatigue testing on simple specimens. Over 50 specimens were tested. The fracture surfaces were inspected using an optical measuring microscope with objective lenses ranging from 5× to 100× magnification. An important efficiency goal of this work was to avoid the use of more expensive observation technologies, like the scanning electron microscope.

2.1 Test Specimen

The specimens were either a dogbone or side-notched geometry per Fig. 1. Military specification processes were used to manufacture the specimens, resulting in anodised (MIL-A-8625 type 1B) and machined (Ra 0.8 µm) surface conditions for the aluminium and titanium alloy materials respectively. No damage tolerance fatigue notch starters were applied, i.e. the specimens were allowed to initiate fatigue cracks representative of aircraft metallic components, which enabled relatively small cracks (down to 0.1 mm) to be considered in this development.

All loadings were applied uni-axially. The stress concentration factor (Kt) for the dogbone and side-notched geometries were 1.08 and 3.4 respectively. This was done to represent the range of stress gradient conditions usually present in aircraft components, such as monolithic bulkheads and fastener holes.

2.2 Materials and Microstructure

Two modern combat aircraft metallic materials were studied: Aluminium Alloy 7050-T7451 6-inch plate (Al7050) and; Titanium Alloy Ti-6Al-4V beta-annealed extra-low-interstitial 4-inch plate (Ti64).

Al7050 is a relatively fine-grained and lower strength material due in part to the larger number of slip planes available in its face-centre-cubic crystalline structure, which also results in a relatively flat fracture surface (Fig. 2). Most currently available marker bands have been developed for Al7050 and Al2024 alloys [2]-[14].

In contrast, Ti64 is a larger-grained and higher strength material due in part to fewer slip planes available in its close-hexagonal-packed crystalline structure. Apart from generally being more resistant to crack progression, Ti64 also results in a relatively rough surface that can make QF very difficult to apply (Fig. 2).

The aim of assessing these two materials was to work toward a single marker design that could be robustly applied to assemblies that may comprise of both aluminium and titanium alloys.

2.3 Flight Load Sequence

The marker load sequences were added to two test flight load sequences: a wing root (WR) and a horizontal tail (HT) bending moment sequence as shown in Fig. 3. Each sequence contained ~70000 turning points (not including marker loads) and represented ~500 flights.

The WR sequence was applied to the dogbone shaped specimens, while the HT sequence was applied to the side-notched specimens. The applied stress levels are summarised in Tab. 1. These stress levels resulted in the specimens failing at about 12000 flights on average, which is representative of combat aircraft damage tolerant structure. Note the yield strength for Al7050 and Ti64 is about 430 MPa and 800 MPa respectively.
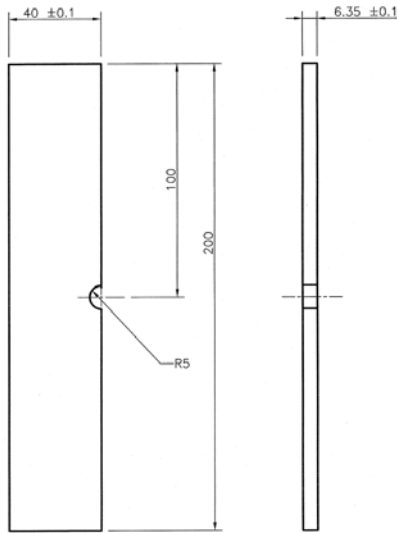
Tab. 1. Summary of peak spectrum Kt-stress applied to the fatigue test specimens.

Flight load spectrum	Specimen Geometry	Peak elastic notch stress, Kt.σ (MPa)	
		Al7050	Ti64
Wing Root	Dogbone	~ 280	~ 650
Horizontal Tail	Side-notched	~ 410	~ 950
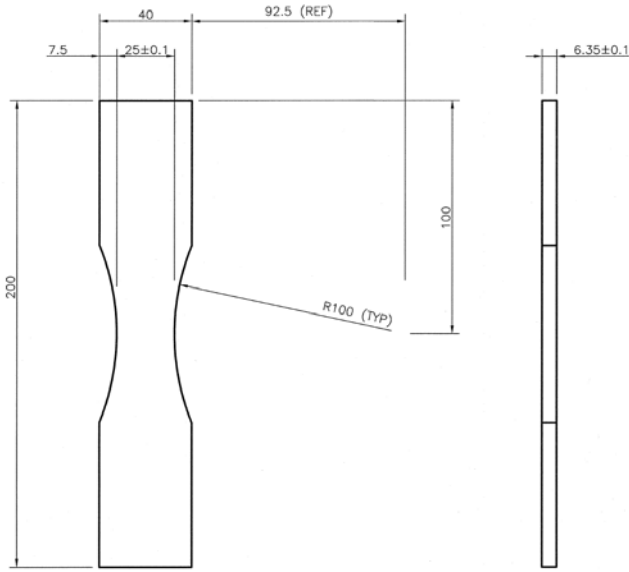
(a) dogbone, $Kt_{net} = 1.08$

(b) side-notched, $Kt_{gross} = 3.4$

Fig. 1. Geometry of the dogbone and side-notched fatigue test specimens (dimensions in mm).
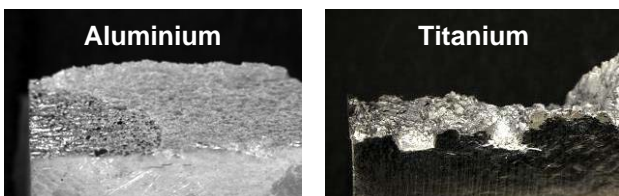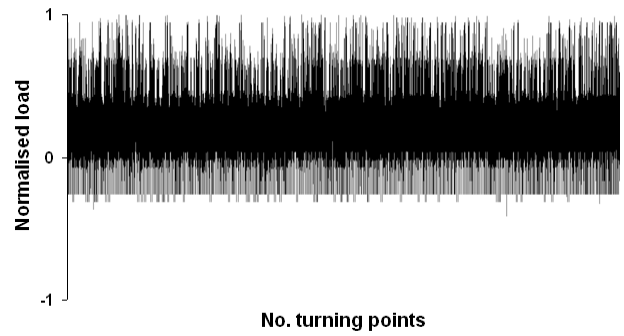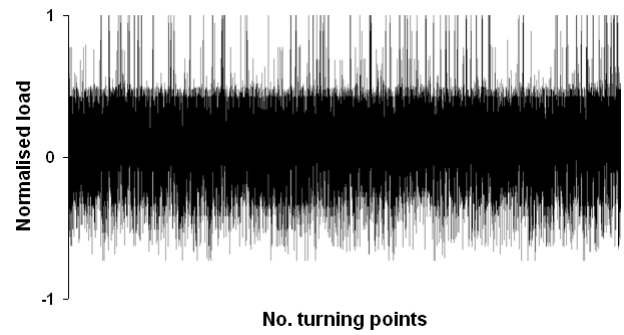

Fig. 2. Comparison of the macro-morphology of fracture surfaces, showing the relative smooth surface of Al7050 compared to the rough surface of Ti64.

(a) Wing Root (WR) sequence

(b) Horizontal Tail (HT) sequence (inverted)

Fig. 3. The normalised flight load sequences used as the basis for the marker development.

3   Marker Band Development

3.1   General Approach

Previous work on aluminium alloy [10] used constant amplitude (CA) loading with relatively small amplitude, high mean load magnitudes (e.g. max/min of 0.7/0.5 of the normalised flight load sequence). This produced reflective markers that contrasted well against the more textured surface inscribed by the variable amplitude (VA) flight loading.

In this work, the main design variables considered for developing a marker for titanium were the magnitudes (max/min) of the CA loading and the number of cycles. The aims were to: (1) grow a microscopically flat, reflective surface that was readily visible under an optical microscope; and (2) minimise the life effect associated with the marker band.

A key constraint was to limit the maximum and minimum loads of the marker to be well inside the bounds of the VA flight loading in order to avoid complex retardation or

acceleration effects on subsequent flight load crack growth rates.

3.2 Marking Titanium

Initial experiments using the WR flight sequence showed that it was possible to mark the Ti64 material. However it required using higher load levels, i.e. max/min of 0.85/0.6 of the peak flight load, compared to 0.7/0.5 for Al7050.

Fig. 4 shows the distinct change in fracture surface morphology between the VA flight loading (rough and darker) and the CA marker loading (flat and reflective), which provides the necessary contrast to locate the markers using an optical microscope. This particular example used a marker consisting of 2000 cycles of 0.85/0.6 loading, with 10 cycles of 0.85/0.05 inserted at the midpoint to help positively identify the marker.

The Ti64 specimens typically produced occasional, short segments that were visible across the crack front. In contrast, the marker bands could usually be identified almost across the entire crack front in Al7050. This difference was attributed to the relatively fewer available slip planes in the titanium crystalline structure, causing only occasional, favourably-orientated grains to be amenable to marking.
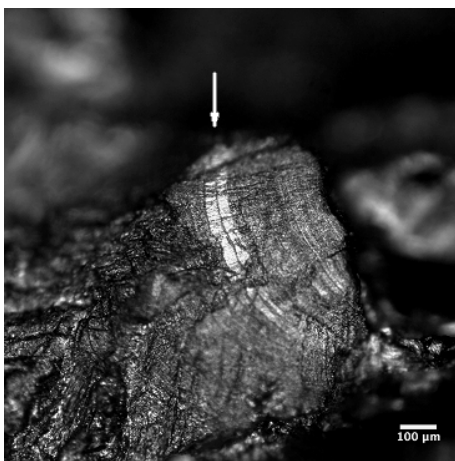

Fig. 4. Clearly visible marker band in a Ti64 specimen.

3.3 Marker Band Size Trials

To determine how small these marks could be made, while still remaining visible, tests were conducted where several different sized markers were inserted into the flight load sequences (WR and HT). The size, or crack progression, under the marker loading was controlled by varying the number of cycles applied. The markers typically consisted of many cycles of 0.85/0.6 to create a flat, reflective surface, and a few cycles of 0.85/0.1 added usually at the midpoint to create contrasting bands to help positively identify the markers.

The WR trial contained three sized markers as shown in Fig. 5. Each of these WR markers contained 5 cycles of 0.85/0.1 at the midpoint. Fig. 6 shows an example Al7050 fracture surface where all markers can be seen together in a single view.

In general, on the Al7050 fracture surfaces the WR markers (a) and (b) were readily visible, however (c) was visible only some of the time. On Ti64, (a) was visible, (b) was sometimes visible, however (c) was rarely found.

The HT trial contained similar markers (4040, 2020 and 1010 cycles) as shown in Fig. 7. Most markers of all three sizes could be found when the crack was larger than ~0.1 mm, indicating that fewer cycles could have been used. Subsequent HT tests that used only 614 cycles were also successful, as shown in Fig. 8.

Based on the WR and HT marker size trials, the minimum practicable limit for identifying a marker band in the Ti64 material was between 600 to 1000 cycles of CA loading with a max/min of 0.85/0.6 of the normalised flight loading.
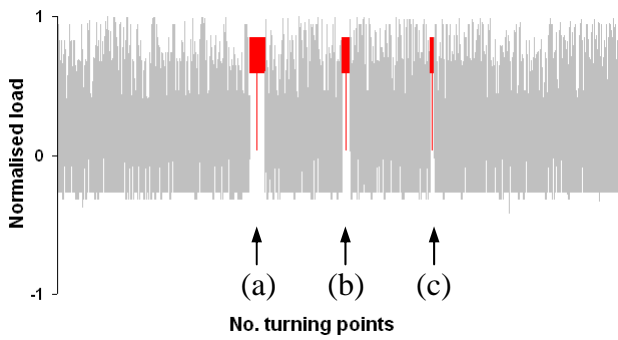
Fig. 5. Plot of the WR flight sequence with three marker band sizes: (a) 1005 cycles, (b) 505 cycles and (c) 255 cycles.
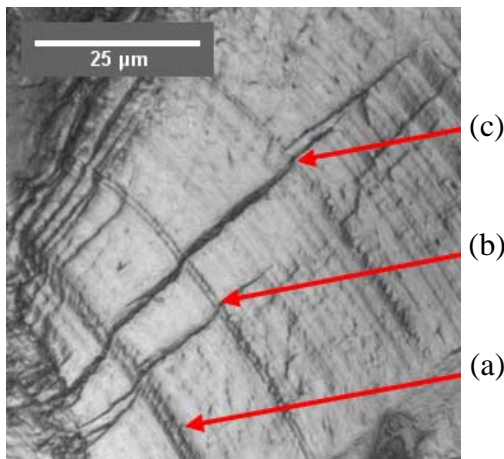

Fig. 6. Example fracture surface of an Al7050 specimen subject to the WR flight loading with three marker band sizes, showing the effect on marker visibility as the number of cycles is reduced: (a) 1005 cycles, (b) 505 cycles and (c) 255 cycles.
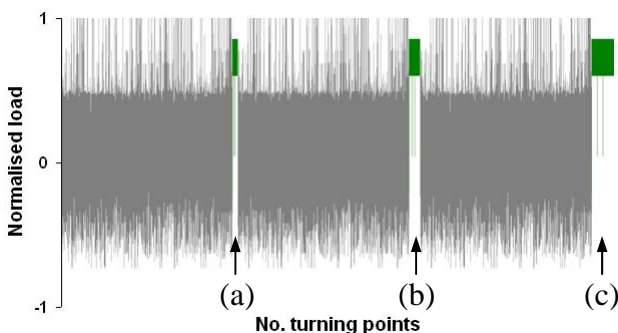

Fig. 7. Plot of three-repeats of the HT flight sequence, each followed by a different sized marker band: (a) 1010 cycles, (b) 2020 cycles and (c) 4040 cycles.
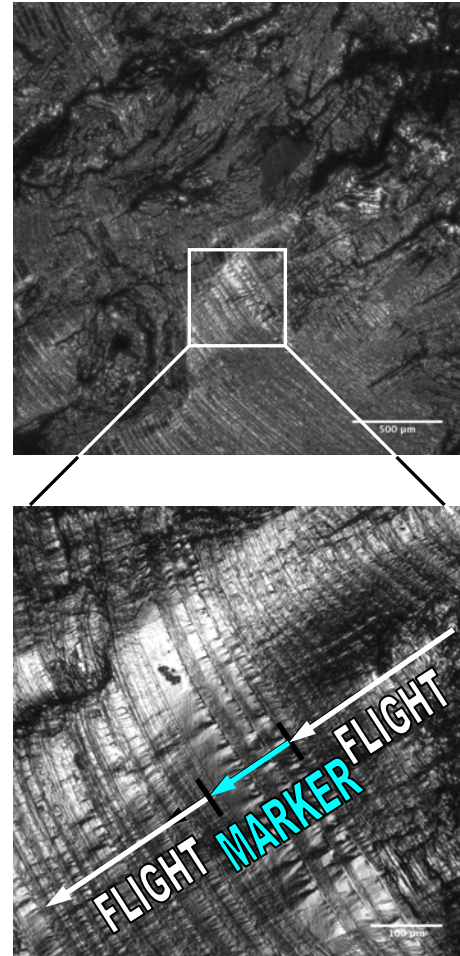

Fig. 8. Example Ti64 fracture surface resulting from a 614 cycle marker band in HT flight loading; showing the highly reflective appearance of the marker against the flight loading. The marker is only occasionally visible in the Ti64 material.

3.4 Marker Band Life Effect

The life effect associated with the 1005 cycle marker in the WR spectrum, and the 614 cycle marker in the HT spectrum, was determined here. Two measures of the life effect were used:

(1) *QF method*, an approximation based on the equivalent 'flight time' associated with the distance that the crack progressed under the marker loading. This method can be readily performed using an optical microscope configured with a calibrated, moveable stage. However, given this method can only be practically applied to cases with marker bands, it can not be used to assess retardation

or acceleration effects (if any) on the flight loading sequence.

(2) *Total-life method*, a statistical comparison of the differences in total failure life between specimens tested with and without marker bands. This method was used to assess if there was an overall retardation or acceleration effect.

3.4.1 QF method

The life effect is expressed here as a percentage of the crack growth due to the marker loading as compared to the growth due to the ~500 flight loading sequence prior to the marker. This approach normalises the life effect against crack size. Interestingly, there was no clear trend with crack size, i.e. the normalised results were independent of the crack size. This allowed the distance ratio to be simply multiplied by the number of flights per load sequence to obtain an equivalent number of flights for the markers.

It was observed on the fracture surface that the thickness of the marker bands varied considerably across the crack front, in particular for the Ti64 specimens. This may be an influence of the variation in crystal-orientation of the many metallic grains intersected by the crack front. Since only 'visible' (i.e. potentially larger) markers were measured by the QF, the results of this method could be biased toward over-estimating the life effect.

Tab. 2 summarises the averaged results. For the WR flight spectrum, the flight time associated with the markers was comparatively small. The averaged results were less than 2% for both Al7050 and Ti64, i.e. the marker load caused a crack progression equivalent to applying less than 10 flights of the VA flight load sequence.

For the HT flight spectrum, only Ti64 specimens were tested. The average result was 9.6% (~50 flights), which was notably higher compared to the result from the WR case, however this was consistent with crack growth analysis predictions for the WR and HT cases. This life effect for the HT case was considered to be moderate, and hence the *total-life method* was applied to assess if the *QF method* over-estimated the life effect.

Tab. 2. Summary of averaged life effect results associated with the marker bands, determined using the *QF method*.

Marker cycles (flight load)	Specimen Geometry	% of flight* spectrum	
		Al7050	Ti64
1005 (WR)	Dogbone	1.3%	1.5%
614 (HT)	Side-notched	not tested	9.6%

*   ~500 flights

3.4.2 Total-life method

Total-life fatigue tests were conducted on Ti64 specimens subjected to the HT loading; 7 specimens *with* a 614 cycle marker included at the end of each ~500 flights, and 7 specimens *without* any marker bands at all. Given that no notch starters were used to help reduce fatigue scatter, the repeats were necessary to obtain a statistically significant comparison.

The results indicate that the marker band had no effect on the total fatigue life, i.e. the difference between failure life populations was statistically insignificant. This also suggests that there was no significant retardation or acceleration effect on the crack growth during subsequent flight loading.

The averaged results are summarised in Tab. 3, however this comparison alone only provides an indication of the actual marker band life effect, since the variance in the total life populations was considerable (the normalised maximum and minimum results were 1.3 and 0.7). Similar future tests for Al7050 are planned.

Tab. 3. Summary of life effect associated with the marker bands using the *total-life method*.

Marker cycles (flight load)	Specimen Geometry	Normalised average total-life	
		Without markers	With markers
1005 (WR)	Dogbone	not tested	not tested
614 (HT)	Side-notched	1.00	0.99

4   Bar-codes

4.1   General Objective

Associating the flight time to a particular marker is usually done by counting all markers backwards from the failure point [10]. However, for cases where some markers cannot be

located, this can add uncertainty for the QF practitioner. This uncertainty was considered to be more significant for Ti64 because the markers that occurred during the final stages of stable fracture were often more difficult to locate, thus increasing the prevalence of missing markers near the failure, i.e. reference point.

Adding uniquely identifiable striation 'counters' to markers has previously been used to improve confidence in determining the crack progression timing [14]-[17]. However it was noted in that work, and also in this study, that the formation of striations was difficult to achieve across a broad range of crack sizes. For example, the individual striations visible in Fig. 9, which were generated using CA load cycles with a max/min of 0.85/-0.3 of the normalised flight load sequence, were only distinguishable at larger crack sizes (> 10 mm). The groups of striations still created dark banding at smaller crack sizes, where the relative thickness of the bands could sometimes be used to ascertain the particular marker code.

This study considered load sequences that would create contrasting (light and dark) bands to inscribe a binary-like 'bar-code' on the fracture surface. It was anticipated that the necessary contrasts could be achieved by altering either the texture or the crack path direction of the fracture surface.
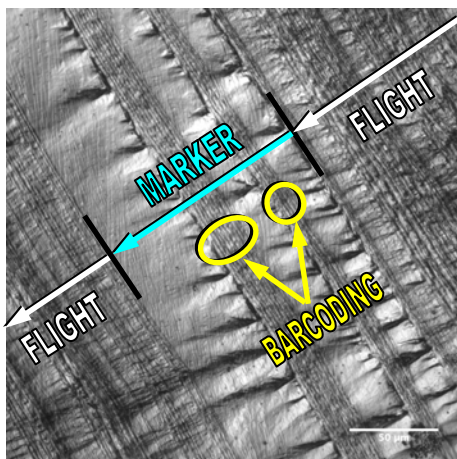
Fig. 9. Early trial (zoomed view of Fig. 8) of a striation-based bar-code marker; showing a group of 4 striations followed later by another group of 8 striations, set within a background of a relatively flat, reflective fracture surface.

4.2 Code Patterning

The maximum number of unique bar-code patterns is limited because a greater number of codes require increasing pattern fidelity, which eventually becomes impractical to distinguish with an optical microscope, particularly at smaller crack sizes.

Hence, it was felt that 8 unique bar-codes, repeated sparingly over the total life (e.g. total of 20-40 markers over the total life) would be sufficient to give the QF practitioner confidence in associating flight times, even in circumstances where a large proportion of the markers appeared to be missing.

An 8-code pattern based on Fig. 10 was selected. Each code comprised of light and dark 'bits' for binary-like identification purposes. The total number of load cycles applied to create the light and dark segments were equal for all 8 codes, in order to maintain commonality on the cycle counts and potential life effects.
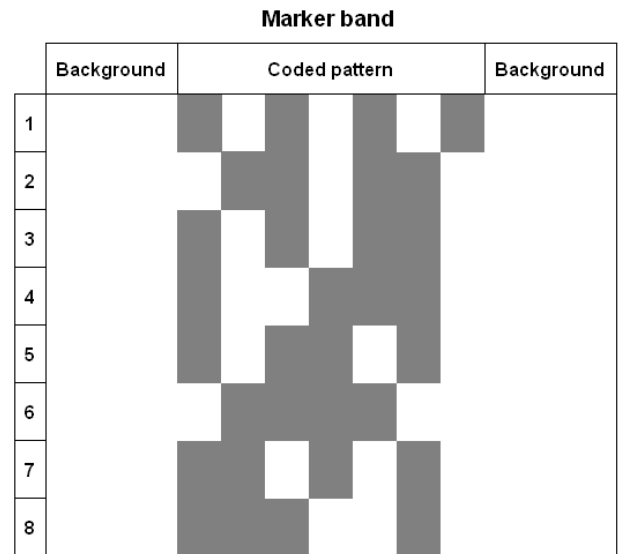
Fig. 10. Concept diagram for 8 uniquely identifiable marker bar-codes, where white regions represent a background flat, reflective fracture surface, and the dark regions represent a visibly contrasting fracture surface.

4.3 Contrast Banding Methods

This study trialed two methods to create contrasting bands against a background flat, reflective fracture surface. The background

loading consisted of ~500 cycles of 0.85/0.6 loading. The first contrasting method was based on *striation-formation* [14]-[17], and the second on *crack-path-alteration* [10]. Each inserted different CA load cycles into the background loading to produce their contrasting effect.

4.3.1   Striation-formation method

The contrasting bands consisted of 10 cycles of relatively high-range (0.85/-0.3) loading to create visible striations. Ideally the individual striations could be distinguished and counted; otherwise these cycles were still anticipated to create relatively dark/textured bands that could be identified by their relative thickness.

The 10 striation-forming cycles were separated into groups by the background loading to create 8 unique codes. An example load sequence (not showing the neighbouring flight loading) is given in Fig. 11. The coded part of the sequences only loosely followed the intent of the patterns in Fig. 10, since the focus here was striation counting rather than light/dark pattern recognition. The equi-spaced single contrasting cycles were inserted to create positional awareness.
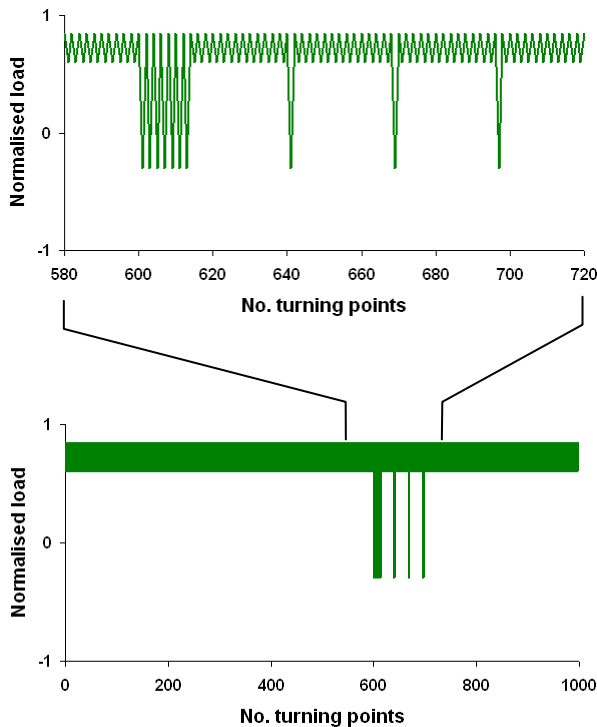

Fig. 11. Plot of an example bar-coded marker based on the *striation-formation* method.

4.3.2   Crack-path-alteration method

The contrasting bands consisted of 80 cycles of medium-range (0.85/0.1) loading to induce a crack path change that would alter the reflective angle of the fracture surface, thus appearing as a contrasting band when illuminated with a directional light source.

The 80 crack-path-altering cycles were separated into groups by the background loading to create the 8 unique codes. An example load sequence is given in Fig. 12. These sequences more closely resemble the patterns in Fig. 10.
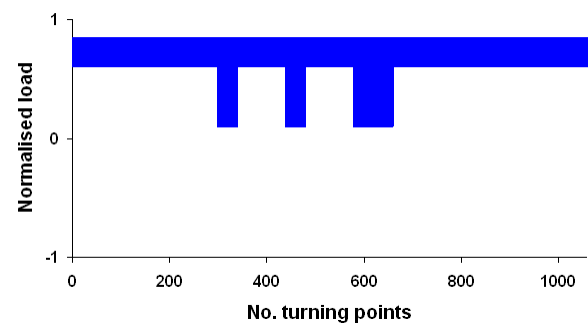

Fig. 12. Plot of an example bar-coded marker based on the *crack-path-alteration* method (code number 3 shown).

5   Results and Discussion

Observations of the resulting fracture surfaces for Al7050 and Ti64 revealed that it was significantly easier to identify markers and their codes based on the *crack-path-alteration* method compared to the *striation-formation* method.

Fig. 13 compares the fracture surfaces of the two types of code for Al7050. However, while these images show similar clarity, the *striation-formation* example is for a much longer crack size (6.0 mm) compared to the *crack-path-alteration* example (1.6 mm).

For Ti64, the *crack-path-alteration* method did not cause crack path changes like those found in Al7050. However, the changes in the CA loading did appear to create contrasting bands. Fig. 14 shows the smallest marker code identified in this work, which was at a crack size of 0.6 mm for the *crack-path-alteration* method. In contrast, the smallest code identified

for the *striation-formation* method was at a crack size of about 4 mm.

The identification of the time progression of the crack growth was substantially improved with the use of bar-codes, especially for the Ti64 material. The 8 unique bar-codes were mostly distinguishable for *crack-path-alteration* method, yet rarely so for the *striation-formation* method.

On average, 24 markers (3 repeats of the bar-code set) were applied to each specimen over the total life. Given that not all codes were independently identifiable, it was felt that increasing either the number of codes, and/or the total number of markers, would make distinguishing the codes more difficult.

The tests conducted herein indicated that the life effect of the markers in both the Al7050 and Ti-64 materials was relatively small. Also, no significant retardation or acceleration effects were observed. More tests are planned to substantiate this for different materials, flight load spectra and stress levels.

The stress levels considered in this study were relatively high in order to represent fatigue critical, damage tolerant structure in a combat aircraft. The marker load sequences developed herein may require adjustment for other stress levels, material types, and flight spectra.

6   Conclusion

The use of quantitative fractography (QF) in the durability and damage tolerance assessment of full-scale aircraft fatigue tests is well proven, however, its use in the aircraft industry is not a commonplace. This is attributed to a combination of: the relatively poor 'mark-ability' of some materials (e.g. titanium); a predisposition for expensive equipment (e.g. scanning electron microscope) and; not the least, the cost and time associated with resourcing skilled QF practitioners.

This study showed that two types of aircraft materials, aluminium and titanium alloys, could be simply marked with the use of special bar-coded marker load sequences, so that only basic QF skills using an optical microscope were required.
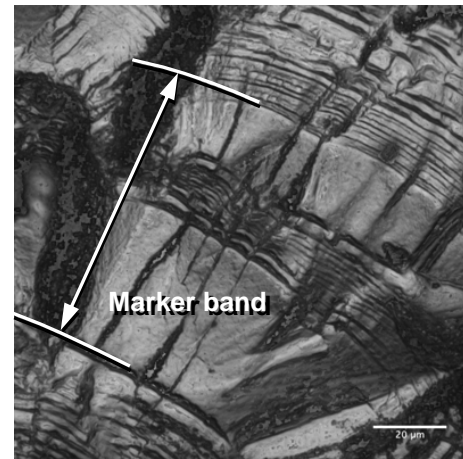
(a)
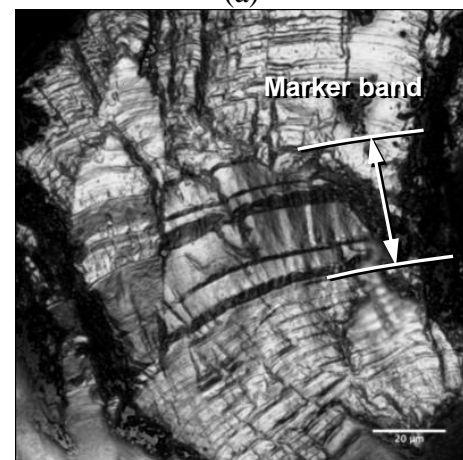
(b)

Fig. 13. Example Al7050 fracture surfaces comparing bar-coded markers produced by: (a) the *striation-formation* method at a crack size of 6.0 mm; (b) the *crack-path-alteration* method at a crack size of 1.6 mm.
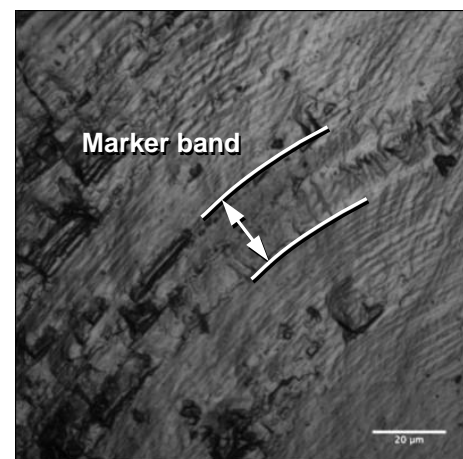

Fig. 14. Example Ti64 fracture surface showing a bar-coded marker based on the *crack-path-alteration* method, visible here as marginally contrasting textures at this relatively short crack size (0.6 mm).

Fatigue tests were used to optimise the marker such that the life effect associated with the marker load sequence was practically insignificant. Importantly, the visibility of the markers was maintained to assure that a broad range of crack sizes could be identified.

The application of a bar-coded marker load sequence technique to element, component and potentially full-scale airframe life substantiation tests would provide additional knowledge about the crack growth conditions at fatigue critical locations in an airframe. This enables a more accurate post-test interpretation (root cause analysis) and improvements to fatigue models; leading to more effective, efficient and timely production changes, retrofits and/or repairs to aircraft structures.

References

[1] Siegl J, Nedbal I and Kunz J. Fatigue crack growth history in damage tolerance design of aircraft structures. *International Journal of Fatigue*, Vol. 31, pp 1062–1067, 2009.

[2] Dainty R. *Use of ''marker blocks" as an aid in quantitative fractography in full-scale aircraft fatigue testing: a case study*. Mecholsky J and Powell S (Editors) *Fractography of ceramics and metal failures*. ASTM STP 827, Philadelphia, pp. 285–308, 1984.

[3] Ragazzo C, Hertzberg R and Jaccard R. A method for generating fatigue marker bands using a constant K_{max} test procedure. *Journal of Testing and Evaluation*, Vol. 23, No. l, pp. 19-26, 1995.

[4] Willard S. *Use of marker bands for determination of fatigue crack growth rates and crack fronts shapes in pre-corroded coupons.* NASA/CR-97-206291, NASA Langley Research Center, Hampton, Virginia, 1997.

[5] White P, Barter S and Molent L. Observations of crack path changes caused by periodic underloads in AA7050-T7451. *International Journal of Fatigue*, Vol. 30, pp 1267–1278, 2008.

[6] Willard S. *A record of all marker bands found in the upper rivet rows of 2 adjacent bays from a fuselage lap splice joint*. NASA/CR-198249, NASA Langley Research Center, Hampton, Virginia, 1995.

[7] Wanhill R and Hattenberg T. *Fractography based estimation of fatigue crack "initiation" and growth lives in aircraft components.* NLR Technical Publication TP-2006-184, National Aerospace Laboratory NLR, Amsterdam, 2006.

[8] Molent L, Barter S, White P and Dixon B. Summary of recent Australian full-scale F/A-18 fatigue tests. *Proceedings of the Eleventh Australian International Aero Space Congress*, Melbourne, 2005.

[9] Klysz S, Lisiecki J, Zasada D, Gmurczyk G, Leski A. ZL-130TCII Fracture surface markers solution for full-scale fatigue test. *Fatigue of Aircraft Structures*, Vol. 1, pp 22-27, 2011.

[10] Barter S, Molent L and Wanhill R. Marker loads for quantitative fractography of fatigue cracks in aerospace alloys. *25th International Congress on Aeronautical Fatigue Symposium*, Rotterdam, 2009.

[11] Rusk D, Arocho A, Pierce J and Abfalter G. *Results of fatigue tests of bare AF1410 steel unnotched flat plates with surface corrosion damage.* NAWCADPAX/EDR-2008/10, Naval Air Systems Command, Structures Division, Patuxent River, Maryland, 2008.

[12] Wanhill R, Hattenberg T, Ten Hoeve H. *Fractographic Examination of Three EGT Rim Specimens.* NLR Contract Report CR96451, National Aerospace Laboratory NLR, Amsterdam, 1996.

[13] Huynh J, Molent L and Barter S, *Fatigue Life Analysis of the F/A-18 Wing Fold*, DSTO-TR-1484, Defence Science and Technology Organisation, Melbourne, 2003.

[14] Conley F and Sayer R. Correlation of predicted and actual crack growth in a transport wing. *Proceedings of the AAIA/ASME 18th Structures, Structural Dynamics & Material Conference*, Vol. A, pp 119-130, San Diego, California, 1977.

[15] Sunder R. Binary coded event registration of fatigue fracture surface. *Proceedings of the International Conference on Digital Techniques in Fatigue*, Editor Dabell B, Society of Environmental Engineers, London, pp 197-218, 1983.

[16] Sunder R. *Compilation of procedures for fatigue crack propagation testing under complex load sequences.* ASTM Special Technical Publication, No. 1006, pp. 211-230, Philadelphia, 1989.

[17] Prakash R and Sunder R. Crack closure stress estimation by decodable marker banding techniques and comparison of results with electron fractographic technique. *Proceedings of the Inst. of Mech. Eng., Part L: Journal of Materials: Design and Applications*, Vol. 221, pp 53-62, 2007.

Copyright Statement